Numerical Analysis by Method of Moment (MoM) of a Rectangular Monopole Antenna with Parasitic Loop Elements

Karlo Queiroz da Costa[1], Victor Dmitriev[1], and Lorena de F. P. de Carvalho[1]
[1]*Engineering Faculdade of Tucuruí, Federal University of Para, Tucuruí, Pará, Rua Itaipu no 36, CEP 68464-000, Brazil, e-mails: karlo@ufpa.br, victor@ufpa.br, lorena.eng@hotmail.com*

Abstract

Ultra wideband systems are characterized by transmitting signals with very short pulses, which are modulated in a range 3.1-10.6 GHz. Examples of these systems are communications, imaging, ranging and localization. Planar monopole antennas are typically used in these systems. This paper presents a numerical analysis by Method of Moment (MoM) of a rectangular monopole antenna with parasitic loop elements to improve the input impedance matching. Details of the mathematical model and discretization of this problem is presented. A MoM code was developed to analyze this antenna. The characteristics parameters calculated are: input impedance, reflection coefficient, distribution of the superficial current density on the antenna, and radiation diagrams. The numerical results obtained were compared with those calculated by the moment-method-based electromagnetic simulation IE3D.

1. Introduction

Planar monopole antennas are generally used in ultra wideband (UWB) systems. These systems have a spectrum ranging from 3.1 GHz to 10.6 GHz with a bandwidth around 106% [1]. Some types of conventional planar monopole antennas are those with rectangular, circular, and triangular shapes [2]. The conventional rectangular monopole antenna has usually a maximum bandwidth around 80% (level −10dB) for a relation W/L=0.7 where W and L are the horizontal and vertical size, respectively, of a rectangular monopole antenna [2]-[4].

Many techniques have been reported to increase the impedance bandwidth of the conventional planar monopoles [5]-[7]. In [5] is presented three compact folded-plate monopole antennas with 1:38 of bandwidth. The authors simulated the antennas by TLM method. In [6] the authors used a modified arrangement to feed a square monopole antenna to increase the bandwidth. The software Ansoft HFSS was used for numerical calculations. They obtained a bandwidth ratio about 1:8.3. In [7] is used a monopole antenna composed by two connected rectangular plates. For this antenna, the return loss level is less then −10 dB from about 3 to 10 GHz. It was used the FDTD method to model this antenna.

In [8]-[10] is used a known technique of combining orthogonal electric and magnetic dipoles to improve the impedance bandwidth of microstrip and linear antennas. This technique is based on minimizing the reactive energy stored in the near zone of the radiator.

This paper presents a numerical analysis by Method of Moments (MoM) [11]-[13] of a rectangular monopole antenna with parasitic loop elements to improve the input impedance matching. In this model, it is used rectangular pulse basis functions for the superficial current and charge density of the antenna. A MoM code written in Fortran was developed for numerical calculations. The characteristics parameters evaluated are: input impedance, reflection coefficient, distribution of the superficial current density on the antenna, and radiation diagrams. The numerical results obtained were compared with those calculated by IE3D [14].

2. Geometry of the antenna

Fig. 1 shows the geometry and reference system of the proposed antennas analyzed in this paper. It consists of a rectangular monopole antenna combined with two parasitic loop elements. The rectangular patch of the monopole antenna has dimensions length L and width W. The connection of this patch with the fed probe is realized by one strip of height H and width s. This strip is positioned at $x=W/2$ of the bottom side L of the patch.

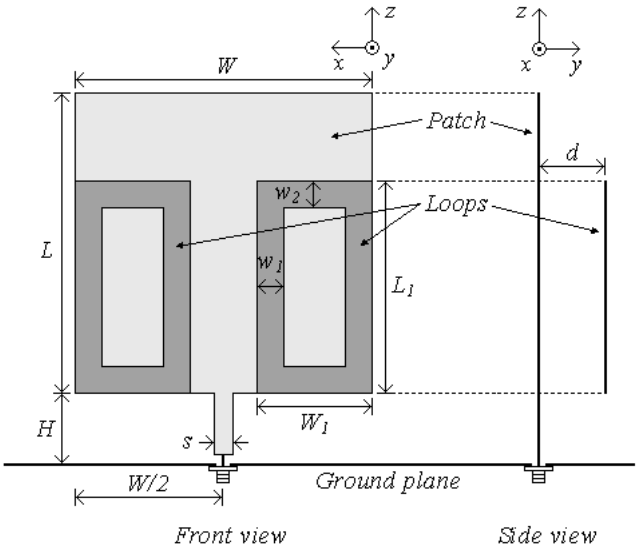

Figure 1. Geometry of the rectangular monopole antenna with parasitic loops elements.

In this figure, the loop elements possess the same geometry, which dimensions L_1 and W_1. The sizes w_1 and w_2 are the widths of the vertical and horizontal strips, respectively, of the loops. These loops are on a parallel plane with respect to the rectangular patch, and the distance between the loops and patch is d (Fig. 1).

3. Mathematical model

3.1. Integral equation of the electric field

The MoM method was used to analyze numerically the antenna proposed in this paper. This method is based in the integral equations of the electromagnetic potentials. For the case of the geometry in analysis, which is only composed by superficial conductors, the following equations were used

$$\bar{E}_r = -j\omega\bar{A} - \nabla\phi \tag{1}$$

$$\bar{A} = \mu_0 \iint_S \bar{J}\frac{e^{-jkR}}{4\pi R}ds' \tag{2}$$

$$\phi = \frac{1}{\varepsilon_0}\iint_S \sigma\frac{e^{-jkR}}{4\pi R}ds' \tag{3}$$

$$\sigma = -\frac{1}{j\omega}\nabla\cdot\bar{J} \tag{4}$$

where $\bar{E}_r$ is the radiated electric field due the current sources localized in free space, $\bar{A}$ the magnetic potential vector, ϕ electric potential scalar, $\bar{J}$ the electric current density (A/m), σ superficial electric charge density (C/m^2), S the surface of $\bar{J}$ and σ, j the imaginary unit, $k = \omega(\mu_0\varepsilon_0)^{1/2}$, ω is the angular frequency (rad/s), μ_0 and ε_0 are the magnetic permeability and electric permittivity in free space, respectively. The following integral equation of the electric field is derived replacing (2)-(4) into (1)

$$\bar{E}_r = -j\omega\mu_0\iint_S \bar{J}\frac{e^{-jkR}}{4\pi R}ds' + \nabla\left[\frac{1}{j\omega\varepsilon_0}\iint_S \nabla\cdot\bar{J}\frac{e^{-jkR}}{4\pi R}ds'\right] \tag{5}$$

3.2. Solution by MoM

The problem to be solved is to find the electric current density ($\bar{J}$) on the conductive surface S of the rectangular patch and loops of the monopole antenna shown in Fig. 1, when a given electric field $\bar{E}_i$ incident in

the antenna. It is considered that the conductors of the antenna are lossless, thus the boundary condition on *S* is $(\overline{E}_r + \overline{E}_i)\cdot \overline{a}_t = 0$, where $\overline{a}_t$ is a unit vector tangential to *S*. The first step to solve this problem given by (5) using MoM is to approach $\overline{J}$ and σ by a finite linear combination in a given basis functions. The expansions used in this paper are

$$\overline{J} = \sum_{n=1}^{N_x-1}\sum_{m=1}^{N_z} J_x^{n,m} P_{J_x}^{n,m}\overline{a}_x + \sum_{n=1}^{N_x}\sum_{m=1}^{N_z-1} J_z^{n,m} P_{J_z}^{n,m}\overline{a}_z \tag{6}$$

$$\sigma = -\frac{1}{j\omega}\sum_{n=1}^{N_x}\sum_{m=1}^{N_z}\left[\frac{J_x^{n,m} - J_x^{n-1,m}}{\Delta x} + \frac{J_z^{n,m} - J_z^{n,m-1}}{\Delta z}\right] P_\sigma^{n,m} \tag{7}$$

where

$$P_{J_x}^{n,m} = \begin{cases} 1 \ , & x_{n-1/2} < x < x_{n+1/2} \text{ and } z_{m-1} < z < z_m \\ 0 \ , & \text{otherwise} \end{cases} \tag{8}$$

$$P_{J_z}^{n,m} = \begin{cases} 1 \ , & z_{m-1/2} < z < z_{m+1/2} \text{ and } x_{n-1} < x < x_n \\ 0 \ , & \text{otherwise} \end{cases} \tag{9}$$

$$P_\sigma^{n,m} = \begin{cases} 1 \ , & x_{n-1} < x < x_n \text{ and } z_{m-1} < z < z_m \\ 0 \ , & \text{otherwise} \end{cases} \tag{10}$$

where N_x and N_z are numbers of divisions along the directions *x* and *z*, respectively, and $\Delta x = W/N_x$, $\Delta z = L/N_z$. Fig. 2 shows the generic grid used to discretize the surface *S* of the rectangular patch and strip in Fig. 1. The functions (8)-(10) are defined inside this grid. The discretization used for the rectangular loops is linear, it means the density current on the vertical and horizontal sides of the loops possess only one component J_z or J_x.

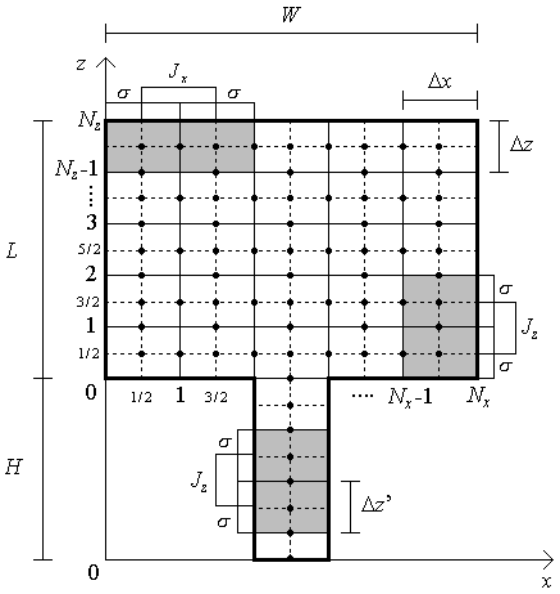

Figure 2. Discretization of the rectangular patch of the antenna shown in Fig. 1.

Fig. 3 shows geometric detail used in each generic current element of index I inside the grid (Fig. 2). In this figure, the direction of P_I^- to P_I^+ is the same of the positive direction of the coordinate systems (+*x* or +*y*). Substituting (6) in (5), applying the boundary condition, and performing the line integral of the resulting equation in segment Δl_J that connect the points P_I^- to P_I^+ is of a generic current element *J*, the following equation is obtained

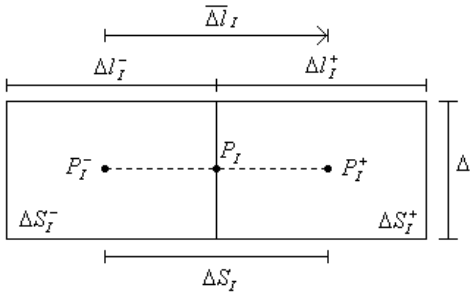

Figure 3. Geometry of a generic element current of index *I* of the grid in Fig. 2.

$$\int_{\Delta l_J} \overline{E}_i \cdot \overline{dl} = \sum_{I=1}^{N_t} J_I \left[j\omega\mu_0 \Phi \overline{\Delta l_I} \cdot \overline{\Delta l_J} + \frac{1}{j\omega\varepsilon_0} \left(\Phi^{++} - \Phi^{-+} - \Phi^{+-} + \Phi^{--} \right) \right] \tag{11}$$

where $N_t = (N_x - 1)\,(N_z) + (N_z - 1)\,(N_x) + N_h + N_{loops}$ is the total number of unknown J_I on the surface of the rectangular patch, where N_{loops} is the total number of current elements of the loops. This current density can be $J_x^{n,m}$ or $J_z^{n,m}$. From the Fig. 1, the following relation can be obtained $H = (N_h - 1)\Delta z' + \Delta z'$. The functions Φ are

$$\Phi = \frac{1}{\Delta l_I} \iint_{\Delta S_I} \frac{e^{-jkR_{IJ}}}{4\pi R_{IJ}} ds' \Bigg|^{P_J} \tag{12}$$

$$\Phi^{++} = \frac{1}{\Delta l_I^+} \iint_{\Delta S_I^+} \frac{e^{-jkR_{IJ}^{++}}}{4\pi R_{IJ}^{++}} ds' \Bigg|^{P_J^+} \tag{13}$$

$$\Phi^{+-} = \frac{1}{\Delta l_I^+} \iint_{\Delta S_I^+} \frac{e^{-jkR_{IJ}^{+-}}}{4\pi R_{IJ}^{+-}} ds' \Bigg|^{P_J^-} \tag{14}$$

$$\Phi^{-+} = \frac{1}{\Delta l_I^-} \iint_{\Delta S_I^-} \frac{e^{-jkR_{IJ}^{-+}}}{4\pi R_{IJ}^{-+}} ds' \Bigg|^{P_J^+} \tag{15}$$

$$\Phi^{--} = \frac{1}{\Delta l_I^-} \iint_{\Delta S_I^-} \frac{e^{-jkR_{IJ}^{--}}}{4\pi R_{IJ}^{--}} ds' \Bigg|^{P_J^-} \tag{16}$$

The variables *R*'*s* in (12)-(16) are the distances between the points (+ or −) of the current element *I* to the points (+ or −) of the current element *J*. If $kR \ll 1$, the following approximations can be used

$$\Phi = \frac{1}{4\pi\Delta l} \left[\Delta l \times \ln \frac{(\sqrt{\Delta l^2 + \Delta^2} + \Delta)}{(\sqrt{\Delta l^2 + \Delta^2} - \Delta)} + \Delta \times \ln \frac{(\sqrt{\Delta l^2 + \Delta^2} + \Delta l)}{(\sqrt{\Delta l^2 + \Delta^2} - \Delta l)} - jk\Delta l \times \Delta \right] \quad \text{if } I = J \tag{17}$$

$$\Phi = \frac{1}{4\pi\Delta l} \frac{e^{-jkR}}{R} (\Delta l \times \Delta) \quad \text{if} \quad I \neq J \tag{18}$$

The left side of (11) means the voltage ΔV applied between the points P_I^- to P_I^+. When (11) is evaluated for $J = 1, 2, ..., N_t$, is obtained one linear system of order N_t. The solution of this system for a given excitation field $\overline{E}_i$, produce the electric current density ($\bar{J}$) on the antenna. The coaxial probe is modeled by a delta gap of voltage $\Delta V = 1$V between the ground plane and the antenna. This delta gap is localized on the first segment of the length *H* near the ground plane (see the Fig. 2).

4. Numerical results

Based on mathematical model presented in Section III, two MoM code was developed in Fortran to analyze the following antennas: conventional monopole planar rectangular and modified monopole planar shown in Fig. 1. The numerical results presented in this section were obtained with the dimensions L=25mm, W=17mm, H=1.25mm, s=1.89mm, L_1=17mm, W_1=8mm, w_1=w_2=2mm, and d=5mm. These antennas (conventional and modified) were simulated by MoM code and IE3D. The numbers of the discretization used in the simulations with the MoM code are: N_x=9, N_z=13, N_h=4, and N_{loops}=56. Others simulations, that are not presented here, were performed to verify the code developed. These results were compared with those of [3]-[4], and a good agreement was achieved.

4.1. Input impedance and reflection coefficient

Figs. 4 and 5 show the results of the input impedance (Z_{in}) and module of the reflection coefficient ($|\Gamma|$), respectively, obtained by MoM code and software IE3D. The Characteristic impedance of the input line feeding is 50 Ohms. In Figs. 4 and 5 is noted a good agreement between the results obtained by the MoM code and the software IE3D. These figures show that the resonant frequency of patch is near the f=3GHz, and the resonant frequency of the loops is near the f=6GHz.

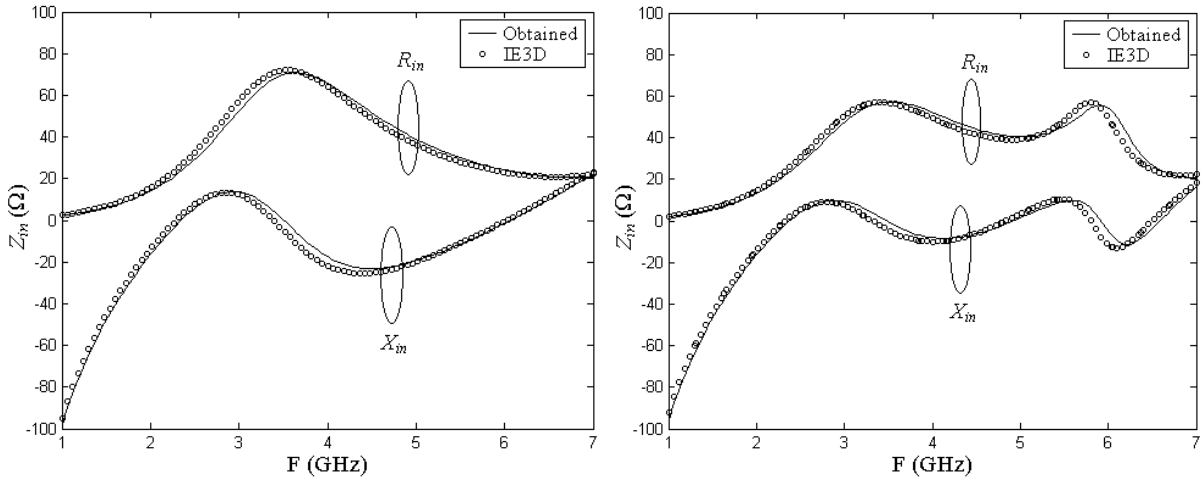

Figure 4. Input impedance of the planar monopoles. (a) Conventional. (b) Modified with loops.

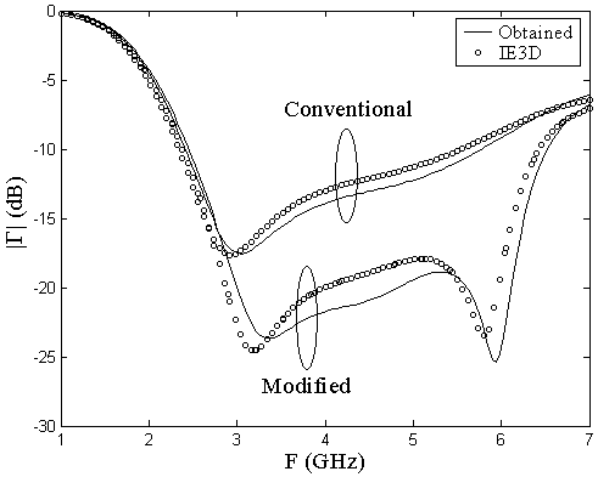

Figure 5. Reflection coefficient of the conventional and modified planar monopoles.

One can observe from these figures that the bandwidth matching of the conventional and modified antenna are approximately 80% and 90% respectively, and the input matching of the modified antenna is better than the conventional antenna. In Fig. 5, the reflection coefficient of the modified antenna is below −15dB in all the bandwidth approximately.

4.2. Current distribution

Fig. 6a shows the module of the current density in each current element of the rectangular patch of the modified antenna in the frequency f=4.54GHz. In this figure, the current elements from 1 to 4 are of the vertical segment H, the segments from 7 to $N_h+N_z\times(N_x-1)=108$ are the component $J_x^{n,m}$, and the others current elements are the components $J_z^{n,m}$. The current element index of $J_x^{n,m}$ and $J_z^{n,m}$ increase from the left to the right, and from down to up, in this order. From this figure it is noted that the module of the components $J_x^{n,m}$ are smaller than the components $J_z^{n,m}$, this means that this antenna possess approximately only vertical polarization.

To observe the variation of $J_x^{n,m}$ near the fed line of the rectangular patch, the Fig. 6b shows the module and phase of this component in the current elements from 5 to 40 in frequency f=4.54GHz. It is observed from this figure the symmetry of the $J_x^{n,m}$ component in the axis x near the point $x=L/2$, and the maximum value of $J_x^{n,m}$ is near this point. The phase is also symmetrical in respect the point $x=L/2$. The module of the components $J_x^{n,m}$ and $J_z^{n,m}$ are shown in Fig. 7, and the Fig. 8 shows in arrows this current density in f=4.54GHz..

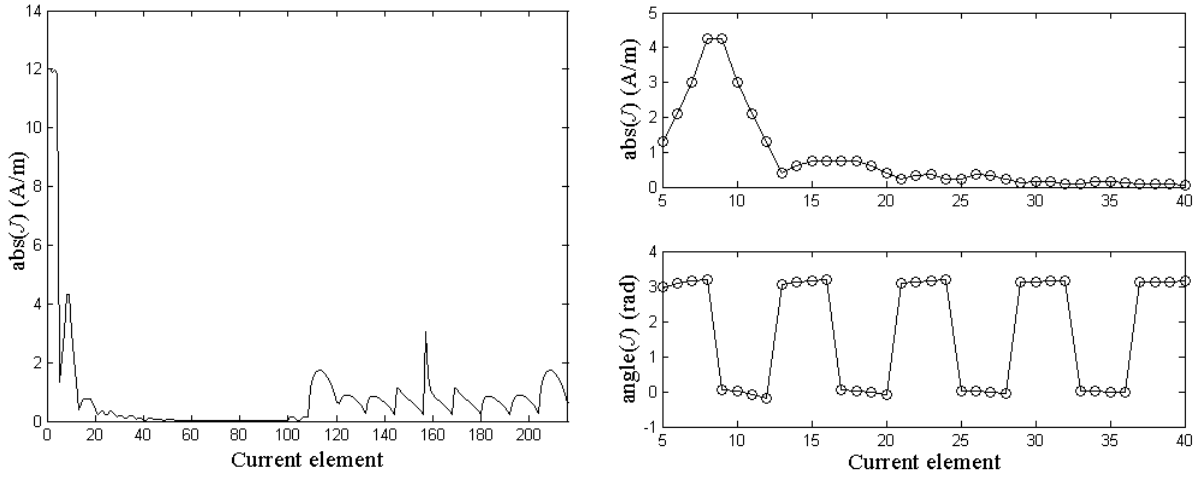

(a) (b)

Figure 6. Variation of the current density on the rectangular patch of the modified antenna versus index of the current elements in f=4.54GHz. (a) index from 1 to 216. (b) index from 5 to 40.

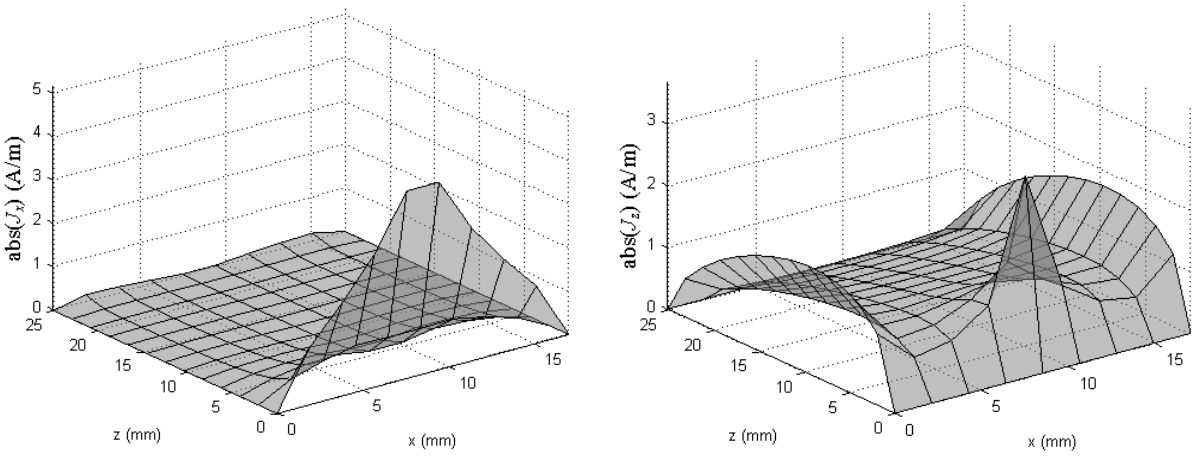

(a) (b)

Figure 7. Module of the current density on the rectangular patch of the modified antenna in f=4.54GHz.

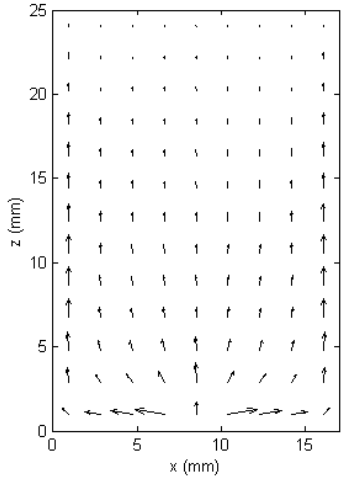

Figure 8. Module of the current density in arrows on the rectangular patch of the modified antenna in *f*=4.54GHz.

4.3. Radiation diagrams

The radiation diagrams of the conventional and modified monopole antenna are show in Fig. 8 and 9 respectively. These diagrams were calculated in the middle of the bandwidth of each antenna, on the planes *xz* and *yz* (Fig. 1).

From this figures, it is noted that these antennas possess only vertical polarization, and the diagrams have approximately ominidirectional pattern. The diagrams for the conventional monopole (Fig. 8) possess symmetry on both planes, and the diagram of the modified antennas on the plane *yz* (Fig. 9b) has asymmetry due the loop elements.

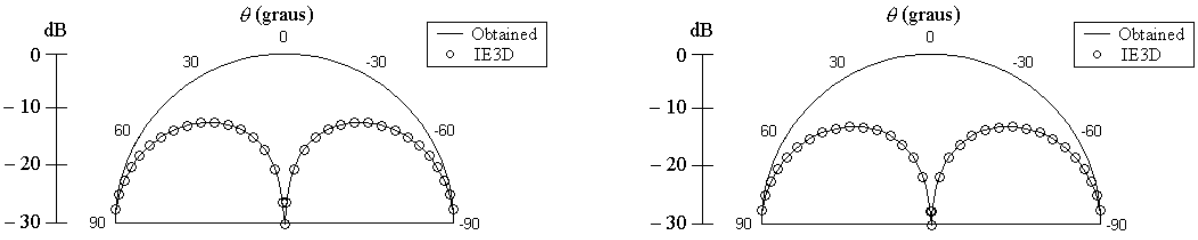

(a) (b)

Figure 8. Radiation diagrams of the conventional rectangular monopole antenna in *f*=4.12GHz. (a) plane *xz*. (b) plane *yz*.

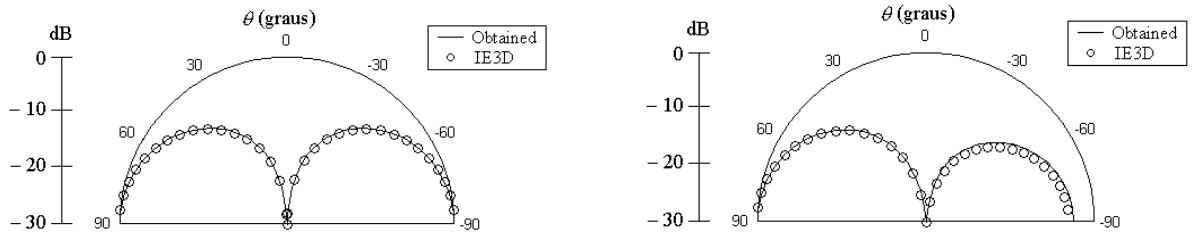

(a) (b)

Figure 9. Radiation diagrams of the modified rectangular monopole antenna with loops in *f*=4.54GHz. (a) plane *xz*. (b) plane *yz*.

5. Conclusions

This paper presented the numerical analysis by Method of Moments (MoM) of a modified rectangular monopole antenna with two parasitic loop elements. Based on MoM model, it was developed a code in Fortran to simulate the antenna. The numerical results obtained from this code are in good agreement with those calculated by the software IE3D and with data in the literature calculated by others techniques. The modified antenna analyzed in this paper presented larger bandwidth and better input matching then the conventional rectangular monopole antenna with same dimensions.

References

[1] Schantz, H., *The Art and Science of Ultrawideband Antennas*, Artech House, Boston, 2005.
[2] Chen, Z. N., and Chia, M. Y. W., *Broadband Planar Antennas: Design and Applications*, J. Wiley & Sons, New York, 2006.
[3] Lee, E., Hall, P. S., and Gardner, P., "Compact Wideband Planar Monopole Antenna," *Electronics Letters, vol. 35* (no. 25), pp. 2157-2158, December 1999.
[4] Ammann, M. J., "Square Planar Monopole Antenna," *1999 IEE National Conference on Antennas and Propagation*, no. 461, pp. 37-40, April 1999.
[5] Valderas, D., Legarda, J., Guitiérres, I., and Sancho, J. I., "Design of UWB Folded-Plate Monopole Antennas Based on TLM," *IEEE Trans. Ant. Propag., vol. 54* (no. 6), pp. 1676-1687, June 2006.
[6] Wong, K.-L., Wu, C.-H., and Su, S.-W., "Ultrawide-Band Square Planar Metal-Plate Monopole Antenna with a Trident-Shaped Feeding Strip," *IEEE Trans. Ant. Propag., vol. 53* (no. 4), pp. 1262-1269, April 2005.
[7] Rikuta, Y., and Kohno, R., "Planar Monopole Antenna with Dual Frequency for UWB System," *2003 IEEE Conference on Ultra Wideband Systems and Technologies*, pp. 176-179, November 2003.
[8] Costa, K. Q., Dmitriev, V., Nascimento, D. C., and Lacava, J. C. da S., "Broadband L-Probe Fed Patch Antenna Combined with Passive Loop Elements", *IEEE Ant. and Wireless Propag. Lett., vol. 6*, pp. 100-102, 2007.
[9] Costa, K. Q., and Dmitriev, V., "Combination of Electric and Magnetic Dipoles with Single-Element Feeding for Broadband Applications", *Microw. Opt. Techn. Lett., vol. 48* (no. 1), pp. 8-12, January 2006.
[10] Costa, K. Q., Dmitriev, V., and Silva, A. O., "A broadband Combined (Linear and Loop) Antenna above a Ground Plane", *2006 IEEE Int. Workshop on Antenna Technology*, New York-NY, March 2006.
[11] Harrington, R. F., *Field Computation by Moment Method*, Macmillan, New York, 1968.
[12] Garg, R., Bhartia, P., Ittipiboom, L., *Microstrip Antenna Design Handbook*, Artech House, Boston, 2001.
[13] Bancroft, R., *Understanding Electromagnetic Scattering Using the Moment Method: A Practical Approach*, Artech House, Boston, 1996.
[14] Software available on http://www.zeland.com/